Published in final edited form as:
Opt Laser Technol. 2012 October 1; 44(7): . doi:10.1016/j.optlastec.2012.03.012.

Depth of focus enhancement of a modified imaging quasi-fractal zone plate

Qinqin Zhang[a], **Jingang Wang**[a], **Mingwei Wang**[a], **Jing Bu**[a], **Siwei Zhu**[b], **Bruce Z. Gao**[c], and **Xiaocong Yuan**[a,*]

[a]Institute of Modern Optics, Key Laboratory of Optical Information Technical Science, Ministry of Education of China, Nankai University, Tianjin 300071, China

[b]Nankai University Affiliated Hospital, Tianjin 300121, China

[c]Department of Bioengineering, Clemson University, Clemson, South Carolina 29634, USA

Abstract

We propose a new parameter *w* for optimization of foci distribution of conventional fractal zone plates (FZPs) with a greater depth of focus (DOF) in imaging. Numerical simulations of DOF distribution on axis directions indicate that the values of DOF can be extended by a factor of 1.5 or more by a modified quasi-FZP. In experiments, we employ a simple object–lens–image-plane arrangement to pick up images at various positions within the DOF of a conventional FZP and a quasi-FZP, respectively. Experimental results show that the parameter *w* improves foci distribution of FZPs in good agreement with theoretical predictions.

Keywords

Fractal zone plate; DOF; Quasi-FZP

1. Introduction

In nature, there are distinctive features of fractal that interest researchers in many fields. In optics, study of fractal has been focused on scattering or reflection from fractional multilayers or super lattices [1-3]. Recent studies are focused on the diffraction of fractal structures by optical elements. Fractal zone plate (FZP) as introduced in [4] is a kind of zone plates with a fractal structure and the corresponding fractal distributions at foci, where irradiance along the optical axis produced by the FZP gives a self-similar profile. An imaging FZP was demonstrated in [5] with advantages of an extended depth of field and reduced chromatic aberration under white-light illumination. The depth of focus (DOF) can significantly be extended due to the fractal distributions at foci. However, DOF is an important property in many optical systems, such as laser ablation, lithography, microscopy and optical data storage, with a requirement of large DOF. Many methods have been proposed for the purpose of increasing DOF, for example annular aperture [6,7], shade mask [8-12], quasi-bifocus [13,14], and image-processing [15,16]. In this paper, we introduce a new parameter in the design of conventional FZPs for DOF extension by a factor of 1.5 or even greater.

*Corresponding author. xcyuan@nankai.edu.cn (X. Yuan).

To further study the effects on axial response, Ref [17] introduced a variable of lacunarity (opaque part) to enhance flexibility in the FZPs design. Based on the variable, a fractal generalized zone plate (FraGZP) [18] was introduced to give another effective parameter ε, a ratio between the period and the transparent portion in a period, for an optimal axial response with a number of modified foci. The ratio ε, however, must be adopted as a positive integer and this requirement more or less restricted design parameters for some optimized intensity distribution (means extension in our paper) cases. In order to improve intensity distributions among the foci, we introduce a new parameter w as a ratio between the transparent and opaque part (lacunarity) in the design of FraGZP to realize the large DOF. It is found that the intensity distribution is improved at foci as DOF is extended simultaneously by controlling w effectively. Detailed parameter selection and analysis are given below.

2. Theoretical analysis

First, we consider the irradiance at a given point on the optical axis with a rotationally invariant pupil function described by $p(r)$. The irradiance, as a function of the axial distance z from the pupil plane, is given by

$$I(Z)=\left(\frac{2\pi}{\lambda z}\right)^2\left|\int_0^a p(r_0)\exp(-i\frac{\pi}{\lambda z}r_0^2)r_0\mathrm{d}r_0\right|^2 \quad (1)$$

where a is the maximum extent of the pupil function. λ is the wavelength of incident light. According to the above formula, we give two different ways to analysis the intensity distribution on the axis. One way is to use a new variable ζ to replace the existing variable r_0 in the pupil transmittance used in producing FZP. The new variable, defined as $\zeta = (r_0/a)^2$, so that we can get $q(\zeta) = q(r_0)$. By employing the normalized axial coordinate $u = a^2/2\lambda z$, we can express irradiance along the optical axis as:

$$I(u)=4\pi^2u^2\left|\int_0^1 q(\zeta)\exp(-i2\pi u\zeta)\mathrm{d}\zeta\right|^2 \quad (2)$$

If the pupil transmittance $q(\zeta)$ has a profile of fractal, the irradiance along the optical axis expressed in terms of the Fourier transform of $q(\zeta)$ will get the self-similar profile. The other way is that the variable is not substituted, which means the pupil transmittance is defined in square radial coordinate. The irradiance along the axis is given in Eq. (1). We will discuss the two cases of the variable with substitution and without in the following parts. The pupil transmittances are both acquired by the cantor set, which is the same as FZPs'. The cantor set has been used to form the fractal profile of FZP following the same procedure given in [3]. In the first stage ($S = 1$) the initial segment is divided into an odd number of segments, $2N - 1$, and the segments in the even positions are removed. For the remaining N segments at the first stage this slicing-and-removing process is repeated in the second stage, and so on. Conventional FraGZPs are modified by controlling the ratio ε. To overcome the stringent requirement of a positive integer, we propose the new parameter w to replace ε in the design of FZPs as described in the introduction. Since, w can be any positive numbers with fractions, it is more flexible to optimize the irradiance of FZPs. According to the process of cantor set; we calculate the period p and give the construction procedure in Fig. 1. In the first stage with $N = 2$ for example, we can get:

$$2\gamma_1+\xi_1=1$$

$$\gamma_1 = w\xi_1 \quad (3)$$

where the period in stage one is given by

$$p_1 = \gamma_1 + \xi_1 \quad (4)$$

In the second stage, the even segments are removed, so in the odd segments we have:

$$2\gamma_2 + \xi_2 = \gamma_1 \quad \gamma_2 = w\xi_2 \quad (5)$$

The period becomes

$$p_2 = \gamma_2 + \xi_2 \quad (6)$$

and so on.

Finally, we get the period of

$$p_S = \frac{w^{S-1} + w^S}{(2w+1)^S} = \frac{w^S(1+(1/w))}{(2w+1)^S} \quad (7)$$

If N is a random integer, the period is

$$p = \frac{w^S(1+(1/w))}{(Nw+(N-1))^S} \quad (8)$$

Based on the analysis, we are able to draw some conclusions below,

- **a.** In radial (r) coordinate, the pupil transmittance and the axial irradiance both have self-similar features, which is in accordance with the FZPs shown in Fig. 2(a), (a′), (b) and (b′). We name the modify FZP as MFraGZP, which has more generalized cases than the FraGZP due to the parameter w.

  If $\gamma = \xi$ or $\xi/\gamma = \varepsilon - 1$, the characters of these cases correspond to FZPs and FraGZPs proposed in [3] and [18], respectively.

- **b.** Except for the above special conditions, we have other choices of w to optimize the axis irradiance of FZPs. This gives more conditions to be used in the design.

After taking into account the dependence of p on the parameter w, the axial irradiance of MFraGZP can be acquired and written in the form

$$I_0 = I_{\mathrm{GZP}}(u, N, S, w) \prod_{i=1}^{S-1} \frac{\sin^2(\pi N u(1+1/w)(w/(Nw+N-1))^i)}{\sin^2(\pi u(1+1/w)(w/(Nw+N-1))^i)} \quad (9)$$

where

$$I_{\mathrm{GZP}}(u, N, S, w) = 4\sin^2(\pi u(w/(Nw+N-1))^S) \frac{\sin^2(\pi M u(1+1/w)(w/(Nw+N-1))^S)}{\sin^2(\pi u(1+1/w)(w/(Nw+N-1))^S)} \quad (10)$$

The term $u = a^2/2\lambda z$ is a normalized axial coordinate; and M is the number of transparent rings.

2) In square (r^2) radial coordinate, the features of this kind of zone plates can be explained by the cantor ring diffractals given by Jaggard [19]. The DOF are improved greatly as shown in Fig. 2(c) and (c'). Consequently, the proposed structure is referred to as quasi-FZP. The different values of w can optimize the axis irradiance of quasi-FZP.

The amplitude transmittances in the two coordinates of binary pupils are then obtained from the rotation of the whole structure around one extreme.

As we know, the FZPs are able to extend DOF under white-light illumination by producing a sequence of subsidiary foci around each major focus following the fractal nature. The subsidiary foci provide an extended DOF for each wavelength that partially overlaps with the other ones, creating an overall extended DOF that is less sensitive to chromatic aberration. To investigate the DOF enhancement feature of the quasi-FZPs, irradiance distributions along the propagating axis as given in Fig. 3 are calculated by the angular spectrum formula [20].

$$U(x,y,z)=F^{-1}\left[F[\mathrm{Pupil}(x,y)]e^{ikz\sqrt{1-\alpha_x^2-\alpha_y^2}}\right] \quad (11)$$

where $F[\bullet]$ and $F^{-1}[\bullet]$ denote the forward and inverse Fourier transform operators, respectively; $Pupil(x,y)$ is the pupil transmittance; α_x and α_y is the direction cosines. We give the axial irradiance provided by an FZP (N=2, S=2) and a quasi-FZP with the same stage and segments (N=2, S=2, w=2) (Fig. 3(a) and (b)) for a=2.5 mm with three different wavelengths in the visible spectrum superimposed, respectively. According to Ref. [5], the focal length of zone plates is inversely proportional to the wavelength. So under different wavelengths light illumination, the subsidiary foci partially overlap with the other ones and create an overall extended depth of focus. The main focal distance in this case is about 20 cm shown in Fig. 3(a′). It can be seen from Fig. 3(a′) and (b′) that the depth of focus of the quasi-FZP has greatly been extended due to superposition of the foci under polychromatic light illumination. Undoubtedly, the FZP also extends DOF shown in Fig. 3(b′), but smaller than the quasi-FZP. From the figures, we can see the focus of quasi-FZP was superposed by different wavelengths and focal distance is up to ~28 cm. However, the focal distance of FZP with different wavelengths only has ~18 cm. In other words; the quasi-FZPs make an improvement of extending DOF by a factor of 1.5 or even greater as shown in Fig. 3(b). Different from FZP, the quasi-FZP has a major focal spot dominating the DOF enhancement, while as the subsidiary foci can work with polychromatic light illumination too.

The aforementioned results indicate that the quasi-FZP can extend DOF effectively. As we know, however, DOF and the resolution are usually traded-off in optical systems. In order to elaborate imaging quality quantitatively, typical imaging evaluation parameters such as super-resolution factor (G), Strehl ratio (S) and sidelobe strength (M) [21-23] of quasi-FZP are studied in detail. The super-resolution factor (G) definition is the ratio between the resolution of the imaging system with the zone plate and the one without any zone plate. The Strehl ratio (S) defined here as the ratio between intensity values of the system with and without the said element. The sidelobe strength (M) is determined by the peak power ratio of the first sidelobe to the main lobe in the focal plane. The imaging device should have a lager value of S and small values of G and M to achieve good quality. The values of S, G, and M versus w are given in Fig. 4. As mentioned before, when $\gamma = \xi$ in radial coordinate corresponding to w=1 in MFraGZPs, the characters of this case are identical to FZPs. The

imaging evaluation parameters of this case (w=1) are shown in Table 1. They are compared with their counterparts of an FZP with N=2, S=2 as shown in the bottom line of the table. It is noted that the factors S and M of quasi-FZPs have a significant improvement than FZPs. Meanwhile; the spot size is remained unchanged in the two cases. In other words, the quais-FZPs have a greater DOF and invariable spot size compared with the FZPs.

3. Experimental results

We experimentally verified imaging capabilities of the quasi-FZP under polychromatic light illumination. We also compared imaging performance between the quasi-FZP and FZP with the same stage and segments. According to the analysis, it is known that a quasi-FZP is composed of an array of concentric rings based on the cantor set. The radii of quasi-FZP can be determined by the periodic formula given in the previous section.

Using the parameters of N=2, S=2 as an example, radii of the rings are r_1, r_2, r_3, r_4, r_5, r_6, and 1, respectively when normalized to the pupil radius. The phase ϕ of each ring gap is set to be 0 or π with respect to the center wavelength λ. In experiments, we fabricated a quasi-FZP with parameters of N=2, S=2 w=2 with the radius 4/25, 6/25, 10/25, 15/25, 19/25, 21/25, 1, respectively and an FZP with N=2, S=2 in a chemically amplified photoresist (AR-N 4340) with a thickness of 833 nm by UV laser direct writing technique (DWL66, HEIDELBERG INSTRUMENTS). The experimental setup is shown schematically in Fig. 5. It is based on a simple object–lens–image plane arrangement and a binary amplitude transmission mask is used as the testing sample. The polychromatic light source (THORLABS, OSL 1-EC Fiber Illuminator) is used for the experiment and the images are detected by a CCD camera (The Chameleon™ USB 2.0 digital video camera) with a pixel size of 3.75 μm × 3.75 μm. The object was illuminated by the polychromatic light and imaged by the plates, then detected by the CCD camera. Feasibilities and applications of diffractive optical elements (DOEs) with incoherent illumination in optical systems have widely been studied, for example Refs. [24,25]. The distance L between the object and the diffractive lens is fixed to 120 mm, and to obtain the defocused images, the distance d from the diffractive lens and the image plane can be adjusted.

To evaluate the size of focal spot of the quasi-FZP, we illuminate the parallel light to the fabricated zone plates and detect the spot size in the focal plane. The measured results of the two elements are shown in Fig. 6. As shown in Fig. 6, the spot size of the quasi-FZP in the focal plane (d=12.0 cm) is about 10 pixels and the same as its counterpart of FZP, while in the defocus planes the spot sizes of FZP become greater than the ones of quasi-FZP in the same distance. Meanwhile, the zero point of FZP appears at 11.0 cm and 12.8 cm around away from the focal plane, which is nearer than the quasi-FZP. It verifies the theoretical prediction that the quasi-FZP has a greater focal depth than the FZP.

To give more intuitive results, we applied a set of letters (EF) in a binary amplitude transmission mask as an object to be imaged at various defocus planes. The letters (EF) were fabricated by mask aligner with the size of 2 mm × 2 mm. In the focal plane (d=8.5 cm), the letters of these two plates are clear. However, the defocused images of FZP at 7.4 cm and 10.2 cm are obscure. As shown in Fig. 7 that the defocused images obtained by quasi-FZP show clear improvements when compared with the counterparts of FZP. It can be seen that the quasi-FZP has a greater DOF than FZP.

4. Conclusion

In conclusion, a new parameter w is considered as a modification to the conventional FZP for optimal distribution of foci and their relative amplitude. Through analysis the pupil transmittance in different coordinates, we compared the MFraGZP and quasi-FZP with the

conventional FZP. It is found that because of the new parameter *w*, MFraGZP covers more generalized cases, including the conventional FZP and FraGZP. Meanwhile, quasi-FZP evolved from the fractal structure improved DOF greatly and verified the imaging capabilities of quasi-FZP with its DOF enhancement experimentally. The optimized design gives rise to a simple and low-cost micro-optical element solution for potential imaging applications with ultra-large-DOF requirement.

Acknowledgments

This work was partially supported by the Ministry of Science and Technology of China under National Basic Research Program of China (9 7 3) grant No. 2010CB327702.

References

1. Sun XG, Jaggard DL. Wave interactions with generalized cantor bar reactal multilayers. Journal of Applied Physics. 1991; 70:2500–7.
2. Jaggard AD, Jaggard DL. Scattering from fracal superlattices with variable lacunarity. Journal of the Optical Society of America A. 1998; 15:1626–35.
3. Jaggard DL, Jaggard AD. Polyadic cantor superlattices with variable lacunarity. Optics Letters. 1997; 22:145–7. [PubMed: 18183130]
4. Saavedra G, Furlan WD, Monsoriu JA. Fractal zone plates. Optics Letters. 2003; 28:971–3. [PubMed: 12836749]
5. Furlan WD, Saavedra G, Monsoriu JA. White-light imaging with fractal zone plates. Optics Letters. 2007; 32:2109–11. [PubMed: 17671552]
6. Welford WT. Use of annular aperture to increase focal depth. Journal of the Optical Society of America A. 1960; 50:749–53.
7. McCrickerd JT. Coherent processing and depth of focus of annular aperture imagery. Applied Optics. 1971; 10:2226–31. [PubMed: 20111306]
8. Ojeda-Castaneda J, Andres P, Diaz A. Annular apodizers for low sensitivity to defocus and to spherical aberration. Optics Letters. 1986; 11:487–9. [PubMed: 19738664]
9. Ojeda-Castaneda J, Berriel-Valdos LR, Montes E. Spatial filter for increasing the depth of focus. Optics Letters. 1985; 10:520–2. [PubMed: 19730471]
10. Ojeda-Castaneda J, Valdos LRBerriel. Arbitrarily high focal depth with finite apertures. Optics Letters. 1988; 13:183–5. [PubMed: 19742021]
11. Indebetouw G, Bai H. Imaging with Fresnel zone pupil masks: extended depth of field. Applied Optics. 1984; 23:4299–302. [PubMed: 18213312]
12. Ojeda-Castaneda J, Berriel-Valdos LR, Montes EL. Line-spread function relatively insensitive to defocus. Optics Letters. 1983; 8:458–60. [PubMed: 19718147]
13. Ojeda-Castaneda J, Diaz A. High focal depth by quasibifocus. Applied Optics. 1988; 27:4163–5. [PubMed: 20539532]
14. Sanyal S, Ghosh A. High focal depth with a quasi-bifocus birefringent lens. Applied Optics. 2000; 39:2321–5. [PubMed: 18345140]
15. Hausler G. A method to increase the depth of focus by two step image processing. Optics Communication. 1972; 6:38–42.
16. Pieper RJ, Korpel A. Image processing for extended depth of field. Applied Optics. 1983; 22:1449–53. [PubMed: 18195985]
17. Monsoriu JA, Saavedra G, Furlan WD. Fractal zone plates with variable lacunarity. Optics Express. 2004; 12:4227–34. [PubMed: 19483968]
18. Yero OM, Alonso MF, Vega GM, Lancis J, Climent V, Monsoriu JA. Fractal generalized zone plates. Journal of the Optical Society of America A. 2009; 26:1161–6.
19. Jaggard, Aaron D.; Jaggard, Dwight L. Cantor ring diffractals. Optics Communications. 1998; 158:141–8.

20. Ersoy Okan, K. Diffaction, Fourier Optics and Imaging. Wiley-Interscience, A John Wiley & Sons Inc;

21. Sheppard CJR, Hegedus ZS. Axial behavior of pupil-plane filters. Journal of the Optical Society of America A. 1988; 5:643–7.

22. Sheppard CJR, Ledesma S, Campos J, Escalera JC. Improved expressions for performance parameters for complex filters. Optics Letters. 2007; 32:1713–5. [PubMed: 17572756]

23. Liu, Linbo; Diaz, Frédéric; Wang, Liang; Loiseaux, Brigitte; Huignard, Jean-Pierre; Sheppard, CJR., et al. Superresolution along extended depth of focus with binary-phase filters for the Gaussian beam. Journal of the Optical Society of America A. 2008; 25:2095–101.

24. Pe'er, Avi; Wang, Dayong; Lohmann, Adolf W.; Friesem, Asher A. Optical correlation with totally incoherent light. Optics Letters. 1999; 24:1469–71. [PubMed: 18079835]

25. Liu JS, Caley AJ, Taghizadeh MR. Diffractive optical elements for beam shaping of monochromatic spatially incoherent light. Applied Optics. 2006; 45:8440–7. [PubMed: 17086253]

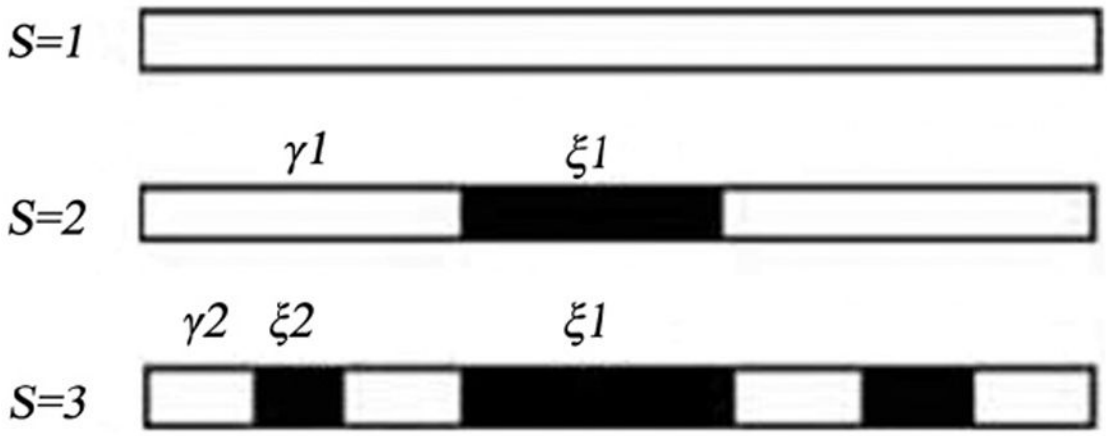

Fig. 1.
The construction procedure of MFraGZP.

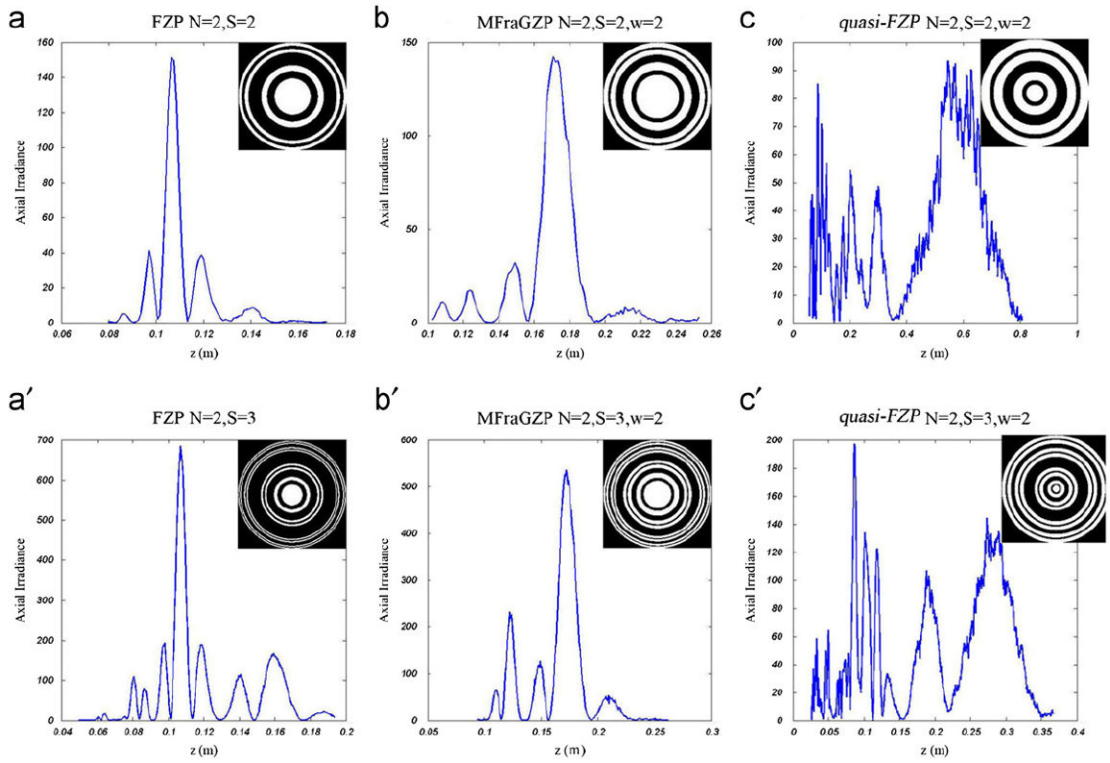

Fig. 2.

The structures and the axial irradiances of the traditional FZP, the MFraGZP (in radial coordinate) and the quasi-FZP (in square radial coordinate). (a), (b), (c) with the same parameters of N=2, S=2, different value of w=1, w=2, w=2 of FZP, MFraGZP and quasi-FZP, respectively. (a′), (b′), (c′) with the same parameters of N=2, S=3, different value of w=1, w=2, w=2 of FZP, MFraGZP and quasi-FZP, respectively.

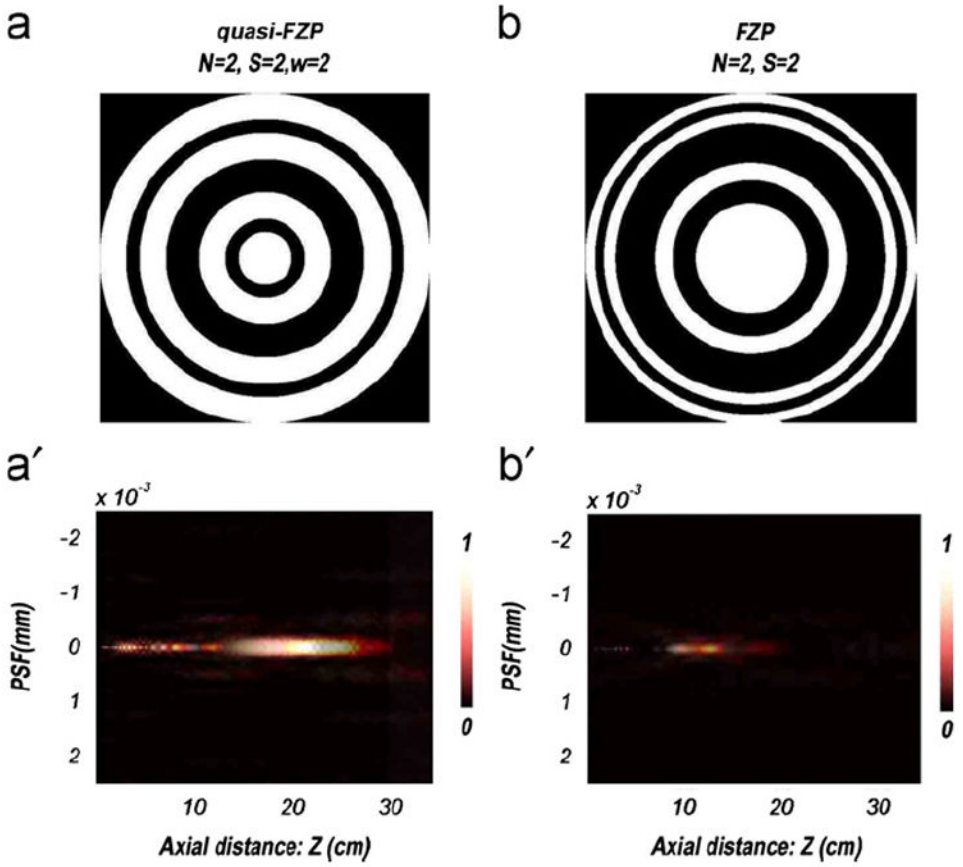

Fig. 3.

The structure of quasi-FZP (*N*=2, *S*=2, *w*=2, Fig. 3(a)) and FZP (*N*=2, *S*=2, Fig. 3(b)) are given. The two dimension axial distributions of quasi-FZP (*N*=2, *S*=2, *w*=2, Fig. 3(a′)) and FZP (*N*=2, *S*=2, Fig. 3(b′)) for *a*=2.5 mm with three different wavelengths of 550 nm, 650 nm and 750 nm superimposed, respectively.

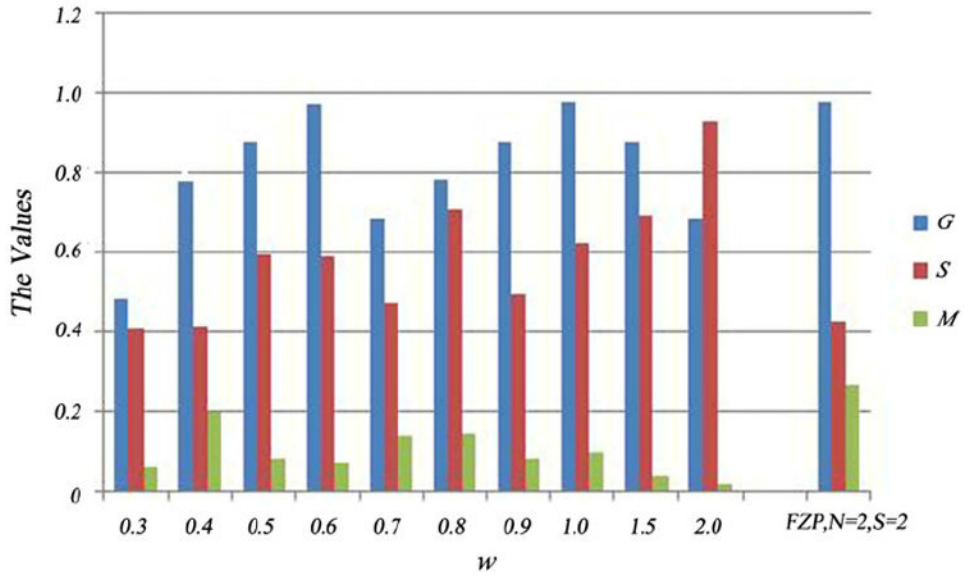

Fig. 4.

Superresolution factor (*G*), Strehl ratio (*S*) and sidelobe strength (*M*) with different *w* of quasi-FZPs and the FZP with *N*=2, *S*=2.

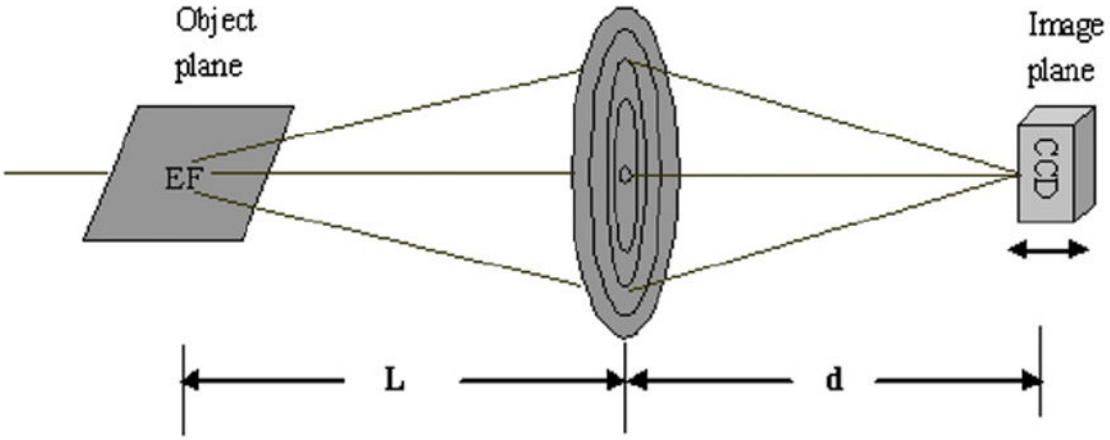

Fig. 5.
The experiment setup of object–lens–image system.

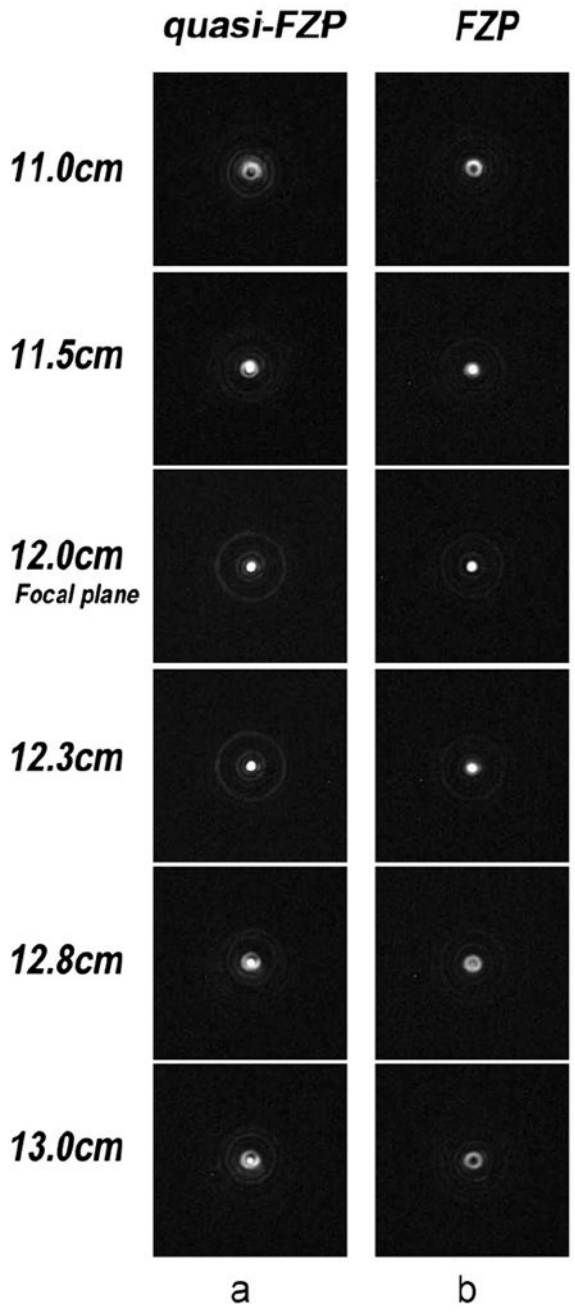

Fig. 6.

The measured spot sizes with different distances in the focus depth of the quasi-FZP (a) and the FZP (b) were obtained. In the front of focal plane (d=11.5 cm, d=11.0 cm), in the focal plane (d=12.0 cm), and behind the focal plane (d=12.3 cm, d=12.8 cm, d=13.0 cm).

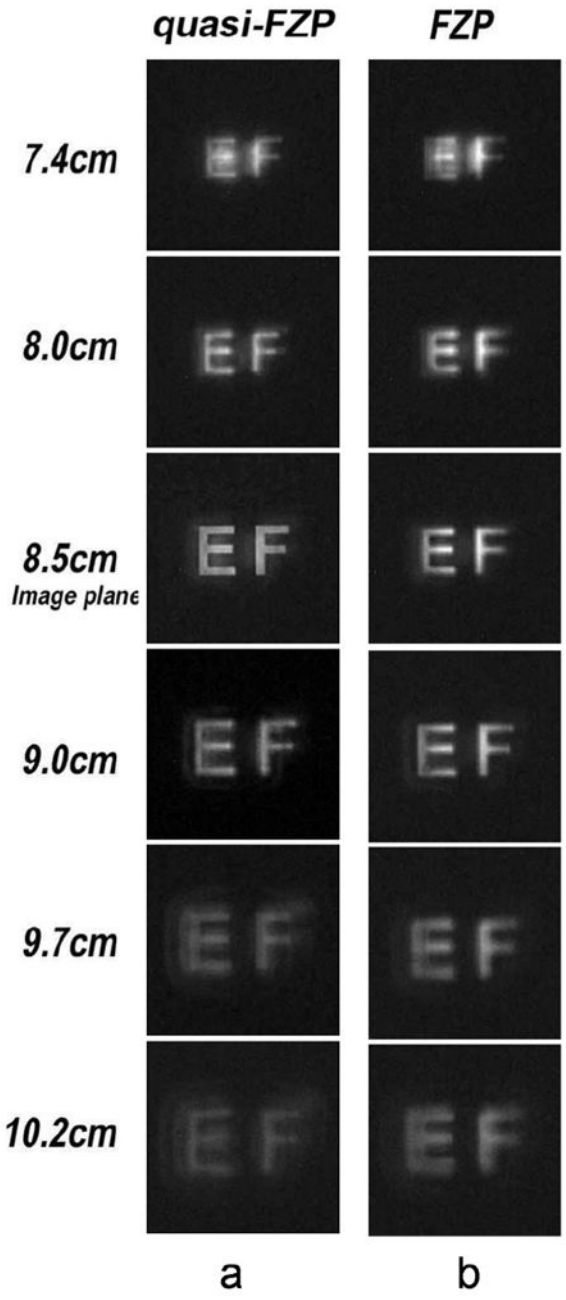

Fig. 7.

Image obtained with the quasi-FZP and with the FZP. Different locations from the image plane were considered: in the front of the image plane (d=8.0 cm, d=7.4 cm), at the image plane (d=8.5 cm), and behind the image plane (d=9.0 cm, d=9.7 cm, d=10.2 cm).

Table 1

MGZP		G	S	M
N=2 S=2	w			
	0.3	0.4847	0.4092	0.0647
	0.4	0.7791	0.4134	0.1983
	0.5	0.8765	0.5949	0.0808
	0.6	0.9739	0.5872	0.0721
	0.7	0.6849	0.4740	0.1384
	0.8	0.7827	0.7098	0.1437
	0.9	0.8806	0.4910	0.0855
	1	0.9784	0.6249	0.0974
	1.5	0.8806	0.6934	0.0393
	2	0.6849	0.9291	0.0161
FZP(N=2, S=2)		0.9784	0.4274	0.2665